Journal of Hydrology (NZ) 40(1): 1-18, 2001

Bedload transport in a meltwater stream, Miers Valley, Antarctica: controls and prediction

R.M. Hawke and J.A. McConchie
School of Earth Sciences, Victoria University, P.O. Box 600, Wellington, New Zealand

Abstract

Bedload transport rates in a meltwater stream in the Miers Valley of Antarctica are highly variable. The major control on the transport of the predominantly sand-sized material is the energy available as a function of discharge; however, the relationship is neither simple nor constant. Change in discharge was able to explain 85% of the variation in bedload transport rates at a site where intensive sampling was undertaken over two 12-hour periods. At discharges below approximately 240 l s^{-1} bedload transport rates vary as a simple power function of discharge. At greater discharges the relationship becomes less regular. The bedform changes from ripples to sand waves and dunes and, as these migrate past the sampling site, they cause wide fluctuations in bedload flux. The higher velocities also exceed the erosion threshold of the sands that make up the banks, leading to undercutting and bank collapse if the ice "cementing" the sands thaws. This results in random pulses of sediment which cause further variation in the actual transport rates. Bagnold's equation, although it predicted the general trend in bedload transport, does not work well in an absolute sense, even in this relatively simple study reach. It under-estimates bedload transport rates by a factor of five. However, once "corrected" for depth and grain size a transport equation based on excess stream power could explain 90% of the variation in the measured bedload transport rate. The slope of this relationship is consistent with that previously reported.

Introduction

Every river has the capacity to erode, transport, and deposit sediment. A wide range of properties control the amount and type of sediment transport, while the mode of transport depends on the interaction of available energy and material resistance. Bedload is that material which moves while in almost continuous contact with the bed: rolling, sliding, or saltating under the driving action of the flowing water. The amount of bedload transport is therefore a function of the energy in the system, both the energy necessary to entrain particles and the energy necessary to transport them. Most often it is assumed that the rate of bedload movement is a function of the transport capacity of the flow. However, in many situations the actual transport rate is also a function of the availability of material (Knighton, 1998).

One control on the availability of bed material that can be moved is the development of an armour layer. While often no more than a grain diameter thick, the armour layer protects the substrate and so limits the supply of sediment able to be moved. This can create conditions in which the actual transport rate is less than the transport capacity of the flow. Even without an armouring layer influencing the fluid–particle interaction, the entrainment of particles is complex. Theoretical conceptualisations of the bedload transport process are often based on observations made either in laboratory flumes, where conditions are contrived, or from a comparatively restricted database (Gomez and Church, 1989). When combined with our incomplete understanding of the principles and mechanisms of entrainment and transport, the variable character of natural streambeds and banks, and the temporal variability of the bedload transport rate, it is not surprising there has been difficulty applying theoretical formulae to "real world" situations (Reid *et al.*, 1997). Accurate field measurements are complicated by the variability of bedload movement and the effect of the sampler on the transport process (Knighton, 1998). In recent years new systems for continuous monitoring of bedload flux have appeared (Garcia *et al.*, 2000; Leopold and Emmett, 1997; Reid *et al.*, 1980; Tunnicliffe *et al.*, 2000); however, it is not always feasible to install these systems in the field. Despite the difficulties with point monitoring of bedload transport, Ryan and Porth (1999) concluded that point estimates using pressure difference samplers, such as the Helley-Smith, could be used to predict annual accumulations of sediment reasonably well.

The Miers Stream in Antarctica is fed almost entirely by meltwater from the Miers Glacier. Streamflow begins towards the end of November, followed by a steady rise in peak daily discharge until the end of December. From the end of December flows decline until they cease completely by the middle of February. Superimposed on this general trend in peak daily discharge are strong diurnal flow fluctuations that are controlled by daily variations in the intensity of direct solar radiation.

The Miers Stream, therefore, offers an opportunity to study bedload transport in a natural system without many of the complications, such as vegetation and precipitation, found in humid areas or those affected by anthropogenic activities. The stream can, in effect, be regarded as a natural flume in which flow varies regularly, and a significant flow event occurs each day. During a summer season the bedload transport rate of the Miers Stream was determined using a Helley-Smith sampler.

The purpose of this study was therefore to extend our understanding of bedload transport processes in the Antarctic (cf. Mosley, 1988) and to test the applicability of Bagnold's (1986) empirical formula. This formula has been relatively successful in predicting fluvial bedload transport in other environments (Gomez and Church, 1989; Martin and Church, 2000).

Study area

The Miers Valley is situated between 78°05'-78°10'S and 163°30'-164°15'E, about 80 km southwest of the New Zealand and United States bases on Ross Island in McMurdo Sound. Although part of the Dry Valley region, the Miers Valley is further south than the better known, and larger Taylor, Wright, and Victoria Valleys. The valley is aligned west-east and has a simple geometry. Two alpine glaciers, the Adams and the Miers, intrude from the west, with their snouts having northerly and southerly aspects respectively (Fig. 1). From these glaciers summer meltwater streams flow down valley to the proglacial Lake Miers. Lake Miers drains to the sea at the head of McMurdo Sound.

The Miers Valley is bounded by ridges up to 1000 m high of Precambrian-Cambrian metasediments, which are faulted and intruded by granite. The bedrock is a biotite-hornblende granite and diorite with numerous lamprophyre and porphyry dykes. On the northern side of the lake there are further metasediments of schist, paragneiss, banded quartzite, and some coarse-grained graphitic marble (Blank *et al.*, 1963). The crystalline rocks are subject to extreme physical weathering, which produces large amounts of sand. This sand is reworked by periodic fluvial, and almost continuous aeolian, processes.

The Adams and Miers glaciers have deposited relatively recent moraines at the head of the valley, while all slopes are mantled with scree deposits. The surface sediments are underlain by permafrost of unknown depth and are subject to frost action during the short summer season. As a result sand and composite wedge polygons cover nearly the entire surface of the valley. This patterned ground is one of the most striking features of the Miers Valley. The valley floor across which the two major streams flow is composed of an armoured pavement that protects more sandy deposits beneath. The armouring layer ranges in size from -4.75ϕ to -1.0ϕ, with a median of -3.5ϕ, and has been formed by the winnowing effect of the wind (Campbell, 1990). The finer sandy matrix beneath, while containing isolated pebbles up to -4.75ϕ in size, is predominantly in the range 0ϕ to 3.5ϕ with a median

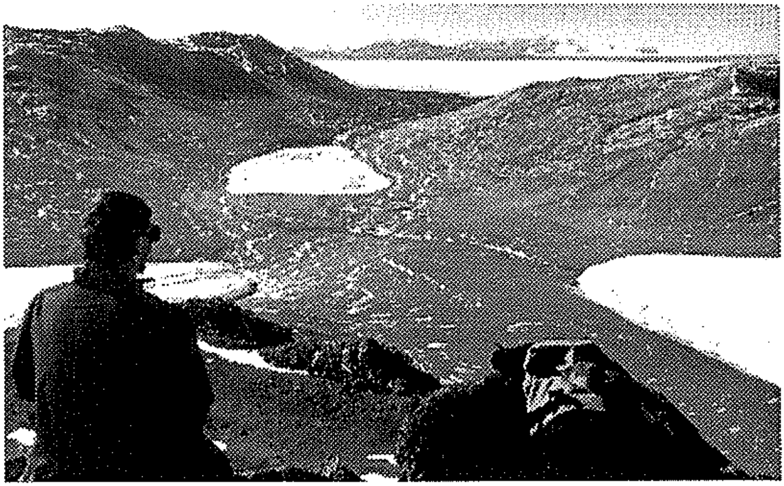

Figure 1 – View looking down-valley towards Lake Miers and McMurdo Sound. The Miers and Adams Glaciers are to the left and right respectively.

of 1.5ϕ. The valley floor is therefore composed of particles with a wide range of sizes with a strongly bimodal distribution. This provides the source of sediment for transport within the rather limited fluvial system.

A single-thread meandering stream (the Miers Stream) is eroded into this material. The stream bed is armoured and directly overlies permanently frozen ground. Because the channel is incised into the permafrost, which is less than 0.3 m beneath the surface, the material forming the banks tends to be "cemented" by ice for much of the year. This improves the stability of these non-cohesive sands and fine gravels. The material forming the banks, while containing a high percentage of fine sands, has a median size of approximately 1.2ϕ, i.e 30% coarser than the median size transported. Over the last 200 m of its course to Lake Miers the stream takes on a braided pattern as it flows across a flat delta. Although the channel is armoured at the start of summer, a range of bedforms develop on top of this layer later in the season as the amount of sand and bedload transport increases. These forms are predominantly sand ripples but include sand waves and dunes, with amplitudes of up to 60 mm, under higher energy conditions.

The Miers Valley has one of the more temperate climates in Antarctica. The valley has warmer temperatures, and as a result more cloudiness, than the main area of Dry Valleys. It has a prevailing easterly wind with speeds during the summer months ranging from 0 to 35 knots and gusts of up to 100 knots. Because the surrounding ranges are relatively low, and the head of the Miers Valley adjoins the Blue Glacier rather than the Polar Plateau, it does not experience the strong katabatic winds common to the north. During the summer seasons for which climate data are available, air temperatures ranged from –8.0 to 6.5°C, averaging around 0°C. Precipitation is minimal (approximately 10 mm per annum) and falls as snow. During the summer any snowfall quickly ablates in the sun because of low relative humidity (McConchie *et al.*, 1990).

Melt-water from the surface of the Miers Glacier cascades down the glacier face to form small streams, which merge to form the Miers Stream approximately 50 m from the snout. For the next kilometre this stream flows in a well-defined channel to the head of Lake Miers. The maximum recorded flow at the gauging station, 200 m downstream from the snout of the glacier, was 0.7 m^3s^{-1} and the water temperature ranged from -1 to 5°C; higher temperatures being experienced under conditions of high suspended load.

Procedure

A 60° flume was installed to provide the hydrometric control for collecting continuous flow data on the Miers Stream (Fig. 2). Stage data were collected every 15 minutes for the 3-month period of summer flow using a Geokon Model 4500 vibrating wire pressure transducer connected to a Campbell CR10 datalogger. Calibration of the transducer-recorded stage against a staff plate gave a coefficient of determination of 0.98. A rating curve developed subsequently had a coefficient of determination of 0.99. This suggests that the discharge data record is very accurate with good resolution.

Sediment transport sampling was carried out using a Helley-Smith bedload sampler with a 63 μm stainless steel mesh bag. While this mesh is significantly smaller than that used in the original Helley-Smith design (200 μm) it is similar to that used by Mosley (1988) in previous work on bedload transport in the Antarctic. Initial concerns that the smaller mesh may restrict flow and cause "back eddies", reducing velocities and diverting sediment away from the sampler orifice, proved unwarranted following field tests discussed later. This type of sampler, although designed in 1971, has been shown to be the best "point-source" bedload sampler, particularly for the sands and fine gravel found in the study site (Thorne *et al.*, 1997). A 'pygmy' current meter was mounted 200 mm in front of the sampler, aligned with the centre of the 80 mm square orifice, to obtain measurements of the velocity of flow transporting the bedload (Fig. 3).

Bedload transport rates were measured at ten cross-sections, over a one-kilometre length of the stream. The sampler was deployed at a number of sites at each cross-section, so that the spacing of samples across the width

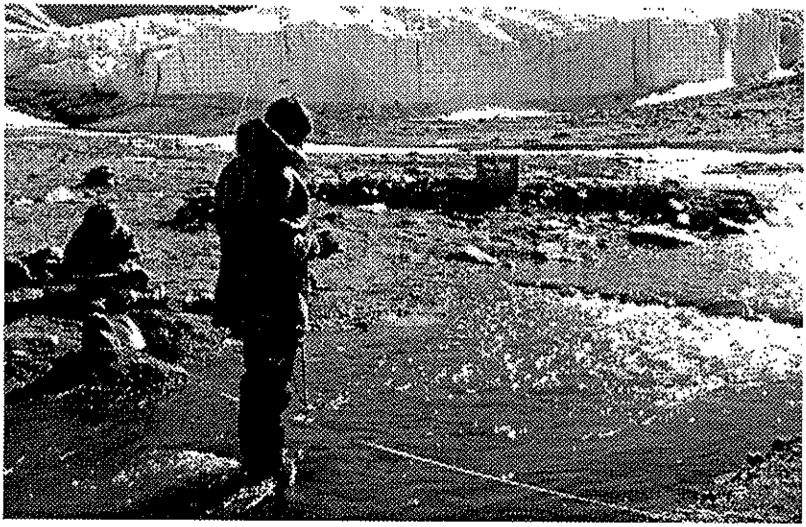

Figure 2 – The hydrometric control on the Miers Stream. In the background are the climate station and Miers Glacier.

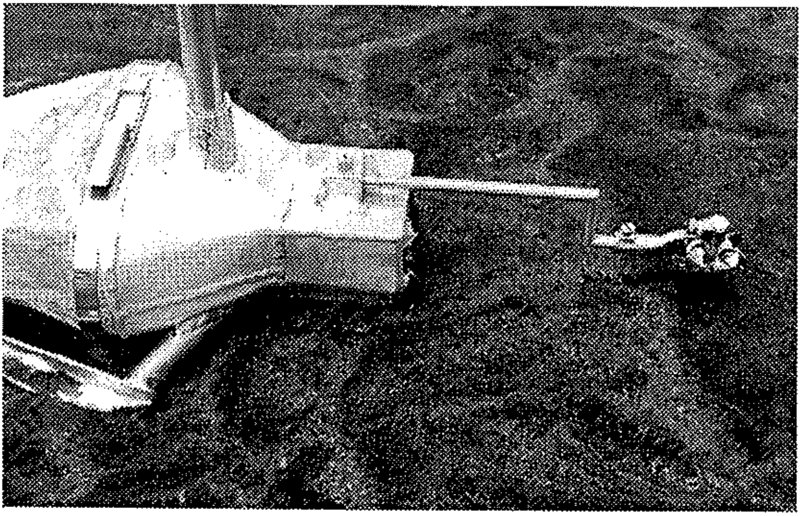

Figure 3 – The Helley-Smith bedload sampler with a 'pygmy' current meter mounted in front. Note the bedforms.

of the stream was approximately 300 mm. At each site the sampler was deployed for 15 minutes, during which time 40-60 g of sediment was usually collected. On one occasion 600 g was caught, but even this mass of material did not appear to disrupt flow through the sampler. In the above manner over 300 point estimates of bedload transport were measured. In addition, the variability in sediment transport was assessed over two 12-hour sampling periods at one site. The temporal and spatial variability in sediment transport, as well as our ability to predict sediment transport, were then assessed.

The placing of any sampler in a stream affects the natural flow patterns, and as a result the potential for transport of sediment. This is true even of the Helley-Smith bedload sampler, which has been shown to create the least disturbance of flow (Helley and Smith, 1971; Reid *et al.*, 1997; Ryan and Porth, 1999). An attempt was therefore made to quantify the effect of the sampler and current meter used in this study on stream flow. Velocity profiles, from the bed to the water surface, were determined using the current meter both with and without the sampler in place. More than 20 vertical profiles of the stream, at different water depths and discharges, were compared. While in general the sampler tended to reduce the velocity, by as much as 20% in the centre of the profile, this effect was not consistent. Reductions in velocity were negligible towards both the bed, where it is expected to find the greatest concentration of bedload, and the surface. Differences between the various profiles were also apparent. Given the size of the sampler orifice relative to the total water depth, the average effect on velocity across the orifice would, however, be significantly less than the maximum point estimates stated above. Although the sampler tended to reduce the velocity of flow slightly, the current meter was in fact recording the actual velocities transporting the sediment that was collected during a particular sampling period. That is, although the velocity may have been reduced, the relationship between velocity and sediment transport recorded at the sampler is correct. In these situations the actual transport rates may be slightly higher than those predicted from these data because of the slightly higher velocities operating under natural conditions. In summary, however, any errors associated with the sampling procedure are relatively minor compared to those through averaging, generalisation, and assumptions inherent in theoretical equations.

The effect of the current meter on the flow around and through the orifice of the sampler was also assessed, using potassium permanganate as a dye tracer. These tests were carried out over a range of flow conditions, particularly at low velocities and shallow depths, when any effect of the current meter is likely to be more significant. While the current meter did cause minor disruption to the flow, and consequently sediment transport, this effect dissipated rapidly, usually in less than half the distance between the current meter and the orifice of the sampler.

As a result of these tests it was concluded that, while the current meter did disrupt the flow, and affect its velocity, these effects were minor. Furthermore, no better alternatives for sampling both velocity and bedload simultaneously were available for this study. The quality of the data used for assessing the validity of bedload equations and developing the relationship between discharge, velocity, and bedload transport is not likely to be significantly affected by the sampling process. However, consideration should be given to this issue when applying these relationships at the field scale.

Bedload in the current study was therefore defined as that material moving within 80 mm of the bed and larger than 63 μm. In reality some material finer than 63 μm was also caught because of the sampler design. Subsequent sediment analysis showed that the material being transported was negatively skewed, mesokurtic, poorly sorted sand with a median size of 1.64ϕ (0.32 mm) (Hawke, 1990).

Regular and repeated stream gaugings allowed the relationships among discharge, channel width, flow depth, and mean velocity to be determined for particular sites. These measurements also allowed an assessment of the variability of hydraulic properties and bedload transport at a point, across a section, down a reach, and throughout the length of the stream. Two 12-hour sampling tests, with samples taken over 15 minutes every 30 minutes, were also undertaken to study the relationship between sediment transport and flow hydraulics, and its variability over time. The cross-section used for these measurements was the same as that used to undertake the gaugings used to rate flow through the flume. As a result stream power could be calculated continuously for flow through the flume, adjusted to the hydraulic conditions at the measurement cross-section approximately 50 m downstream.

Results

Bedload transport

Figures 4a and b show typical daily discharge and bedload transport hydrographs for the Miers Stream. Flows are very low each day until approximately 0900 (NZST) when sunlight starts to strike the glacier. This increases melt and therefore streamflow. Flows then rise rapidly to a peak discharge at around 1400 (NZST) before decreasing through the evening and early morning until the sun starts to strike the glacier again.

Data from the two 12-hour bedload sampling periods show that the Miers Stream displays considerable temporal variability in sediment availability, and consequently bedload transport rates. For periods the stream sediment

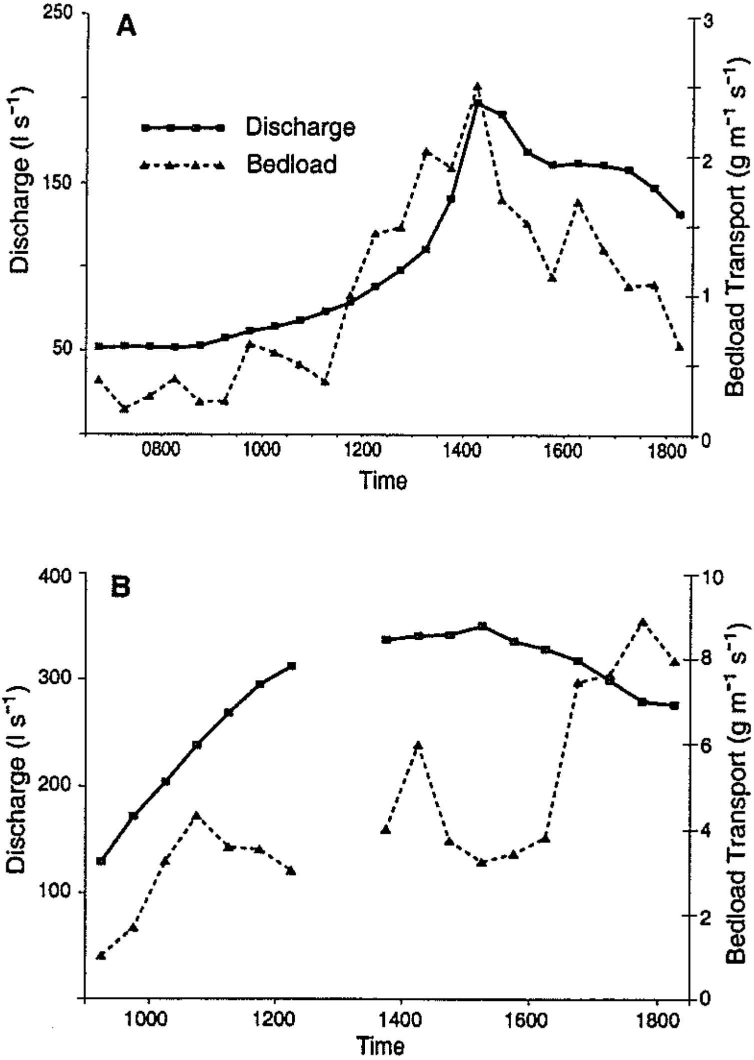

Figure 4 – Water discharge and bedload transport hydrographs for the Miers Stream determined over two intensive sampling periods. (A) Bedload transport changes in "sympathy" with discharge. (B) Both discharge and bedload transport are higher than in (A) but the correlation is weaker.

supply is markedly limited, with troughs apparent in bedload transport rates. Figure 4a suggests that sediment transport is strongly controlled by discharge, as the peaks in the two variables coincide and the bedload transport rate changes in sympathy with discharge. However, Figure 4b, showing data collected 11 days later at the same site, shows a completely different pattern. On this occasion bedload transport is highly irregular, with several peaks and troughs in bedload transport during the diurnal flow cycle.

Bivariate plots (Figs. 5a, b, and c) of the data highlight the differences in the pattern of bedload transport between the two intensive sampling periods. Figure 5a shows an increase in bedload transport with increasing discharge on the rising limb of the hydrograph, but sediment supplies are then depleted, limiting bedload transport. Figure 5b shows the opposite effect, with more sediment apparently becoming available during the falling limb of the hydrograph, leading to significantly higher bedload transport rates. To help overcome the effects caused by the different ranges in discharge the two datasets were combined.

The combined data set (Fig. 5c) shows that a change in the bedload transport relationship occurs at discharges above approximately 240 l s^{-1}. At lower discharges a simple power relationship, based on discharge, can be used to explain 77% of the variability in the bedload transport rate. While size data are not available for both sampling periods, the sediment size characteristics for material transported during the first run were consistent throughout the entire 12-hour period (median = 1.64ϕ, mean = 1.60ϕ, std. dev=0.2ϕ (Figs. 6a and b)). This, combined with sediment size characteristics from samples collected at higher discharges at other sites, suggests that the nature of the material transported did not change during the two events. That is, variation in sediment size was not a significant control on the variation in bedload transport rate. In this situation availability of material must therefore largely control the variation in bedload transport rate about the mean correlation with discharge.

Sediment supply

Using the gauging data from the same site, a discharge of 240 l s^{-1} corresponds to a mean velocity of 0.56 m s^{-1} . From previous studies and theoretical considerations of channels composed of material similar to that in the study area, and with a similar depth, the bedform of sands changes from ripples to sand waves and dunes when velocities exceed approximately 0.5 m s^{-1}. This change in bedform leads to the bedload transport rate past a particular cross-section becoming highly variable. Sampling of a wave or dune trough results in an apparent reduction in bedload transport rate while sampling a crest produces peak transport rates. The migration of bedforms over the armouring layer past the sampling site therefore produces pulses in the measured

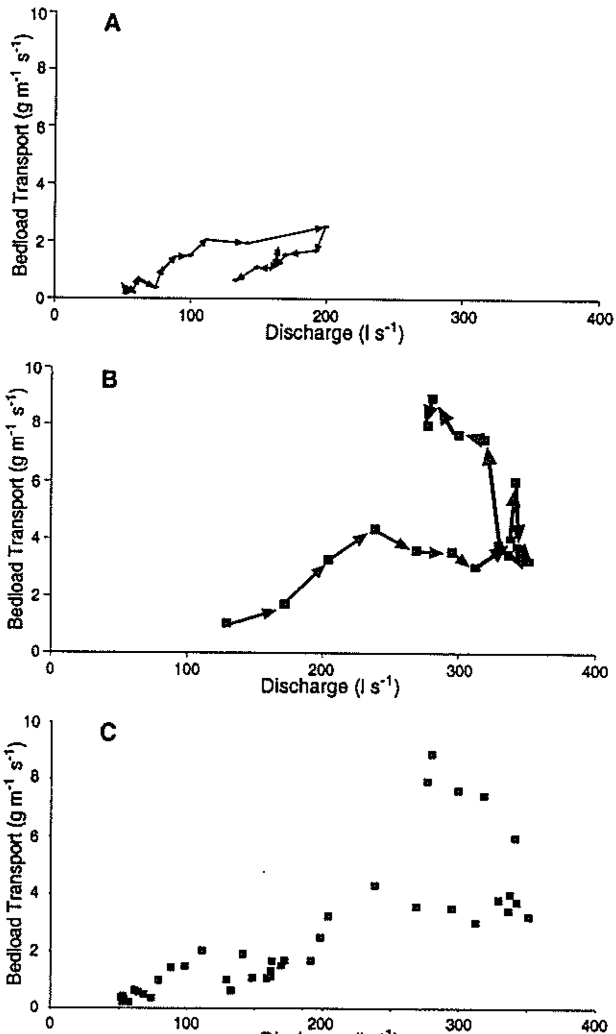

Figure 5 – The relationship between discharge and bedload transport rates over two 12-hour sampling periods. (A) Sediment availability is depleted during the rising limb of the hydrograph leading to a decrease in bedload transport. (B) More sediment becomes available during the falling limb leading to a rise in bedload transport. (C) For the combined data set a considerable change in the bedload transport – discharge relationship appears to occur at flows above 240 l s^{-1}.

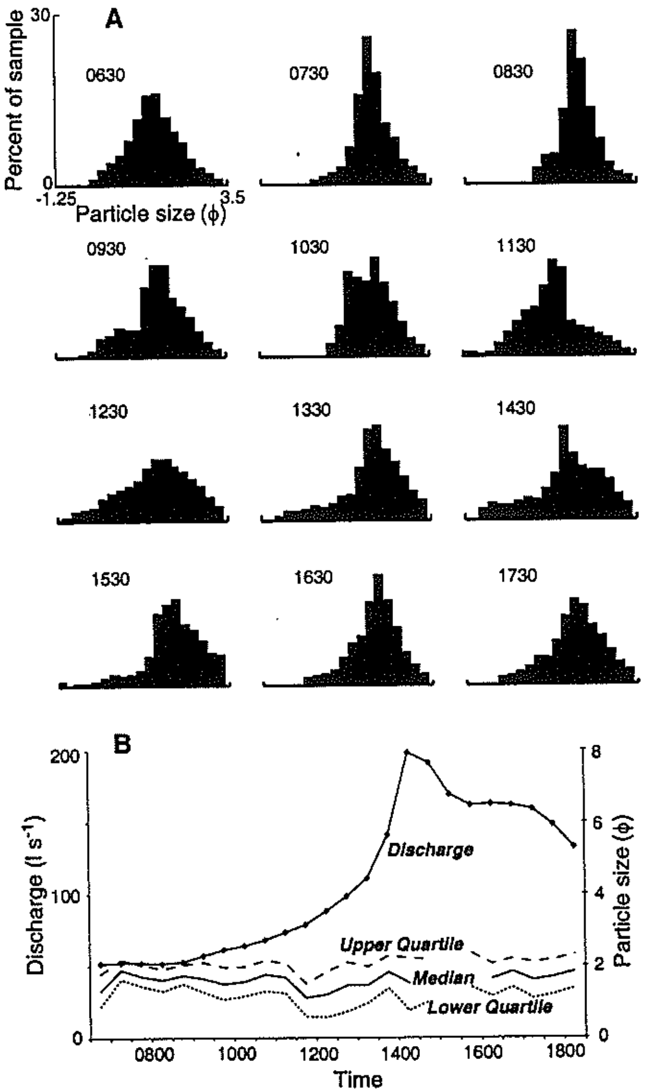

Figure 6 – Bedload characteristics over a 12-hour sampling period. (A) Frequency distribution plots show little change in the characteristics of the bedload despite the four-fold increase in discharge. (B) No significant change occurs in any of the statistical summaries of the particle size distributions.

bedload transport rate and a high degree of scatter in any derived relationship. This observation is similar to that made by Gomez *et al.* (1989) and might be one explanation for the high degree of scatter found at higher velocities (Fig. 5c).

At the higher velocities, not only does the bedform change but the banks become more susceptible to erosion. While the bank material is armoured at the surface by a layer of coarse lag material, this provides no protection to the underlying sands when the banks are incised or undercut. What does provide protection is the fact that the banks are usually "cemented" by ice from either permafrost or water previously drawn by capillary action from the stream. However, depending on aspect, the position of the sun, and on occasion ambient air temperatures, some lengths of the banks periodically thaw. When this happens the banks are easily eroded and collapse, providing sediment directly to the channel. While the median grain size of the bank material is 30% larger than the bedload that was sampled, considerable volumes of readily transportable particles are present. This enhances the variability in sediment supply and consequently bedload transport rates past the cross-section where the measurements were made. These pulses of sand also compound the change in bedform discussed above by adding finer material that can move over any armouring layer.

While these conclusions are valid for the two intensive sampling periods the question remains as to how representative they are for the entire stream system. This was assessed in two ways. First, the bedload transport rate was measured at ten sites over the full length of the Miers Stream. While there is considerable scatter about the discharge–bedload transport rate relationship, the data collected from the two 12-hour sampling periods is consistent with that collected from all the sites (Fig. 7). The anomalous points, with very low bedload transport rates at higher discharges, are all from either the site just below the flume, which occasionally traps some sediment, or where the Miers Stream begins to flow over the delta at a reduced velocity. Second, at each site the bedload transport rate was measured at a number of positions spaced 300 mm apart across the width of the cross-section. The range in bedload transport rates at specific sites across the channel was always within 25% of the mean value for the section.

Theoretical model

The above dataset was also used to test the adequacy of selected theoretical bedload transport models. Most bedload transport equations are based on hydraulic considerations and account for only the interaction of the flow with the channel bed material. In addition, most equations assume that sediment transport is a function of the excess of some flow quantity above a threshold value. The list of variables thought to influence sediment transport

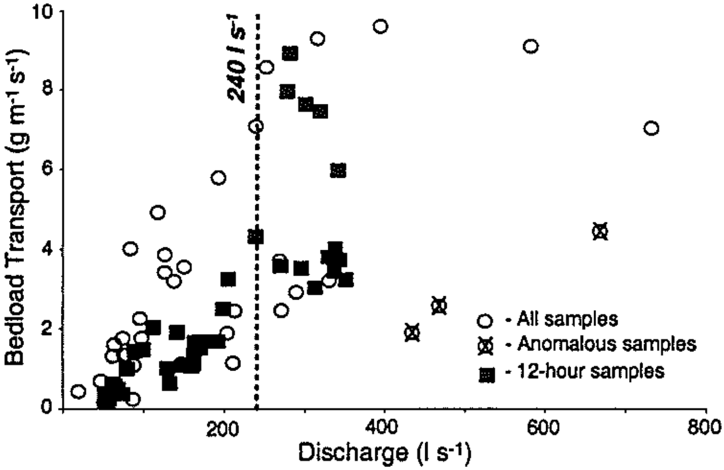

Figure 7 – The relationship between bedload transport and discharge for data from 10 sites over the length of the Miers Stream (1 km).

includes: flow properties (discharge, velocity, width, slope, resistance, flow depth); fluid properties (kinetic viscosity, density, temperature, washload concentration); sediment properties (density, size, sorting, shape); and other properties (gravity, planform geometry). However, conditions such as those in the Miers, i.e. a narrow range of both flow conditions and sediment size, simplify the problem (Knighton, 1998). Given that changes in discharge could be used to explain 77% of the variability in the bedload transport, over the entire range of flows experienced at the 10 sites on this stream, a "stream-power based" relationship was considered most appropriate. Rather than discharge being the control on sediment transport, Gomez and Church (1989) suggested that the approach of Bagnold (1980 and 1986) looked the most promising for bedload prediction, i.e. the bedload transport rate is a function of excess stream power. They also introduced the ($\gamma_s/\gamma_s-\gamma$) term to convert immersed weight to dry weight, thus:

$$Q_s = \frac{\gamma_s}{\gamma_s - \gamma} Q_{sr} \left[\frac{\omega - \omega_0}{(\omega - \omega_0)_r} \right]^{3/2} \left(\frac{Y}{Y_r} \right)^{-2/3} \left(\frac{D}{D_r} \right)^{-1/2}$$

and $$\omega_0 = 5.75[0.04(\gamma_s - \gamma)]^{3/2} \left(\frac{g}{\rho} \right)^{1/2} D^{3/2} \ln\left(\frac{12Y}{D} \right)$$

reference values: $(\omega - \omega_0)_r = 0.5$ $\quad Y_r = 0.1$

$D_r = 0.0011$ $\quad Q_{sr} = 0.01$ (Bagnold, 1980)

where:

Q_s = specific bedload transport rate
γ_s = unit weight of sediment
γ = unit weight of water
ω = specific stream power
ω_0 = critical specific stream power
Q_{sr} = reference specific sediment transport rate
ω_r = reference specific stream power
ρ = density of water
Y = water depth
Y_r = reference water depth
g = acceleration due to gravity
D = characteristic sediment size (usually assumed to be the D_{50})
D_r = reference characteristic sediment size
u = mean velocity

Using data from this study, the observed bedload transport rate is strongly correlated with the rate computed using the Bagnold equation, but it is substantially lower (Fig. 8a). The Bagnold equation over-estimates the transport rate by a factor of five. An alternative formulation of the above transport equation (Bagnold, 1986) is to 'correct' the observed bedload transport rate with reference to depth and sediment size and then compare this to 'excess stream power', i.e.

$$Q_s = Q_s\left(\frac{Y}{Y_r}\right)^{2/3}\left(\frac{D}{D_r}\right)^{1/2}$$

where:

Q_s' = 'corrected' sediment transport rate, the observed bedload transport rate adjusted to a common flow depth and grain size

The log-log plot of the 'corrected' observed bedload transport rate against excess stream power shows that stream power can be used as a good predictor of bedload transport rate, particularly at lower discharges and velocities (Fig. 8b). The slope of the relationship is similar to that found by others (Martin and Church, 2000).

Short-term fluctuations in sediment movement, sediment supply constraints, the movement of sediment as pulses, changes in bed morphology and dynamics, and distortions caused by the armouring of the bed, however,

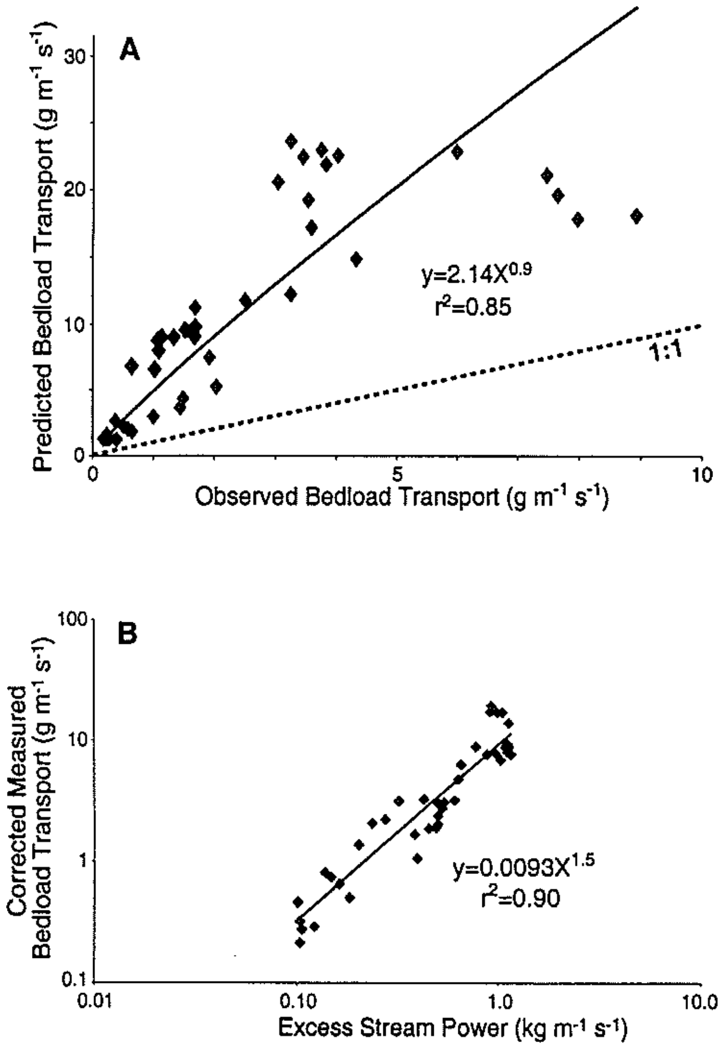

Figure 8 – (A) There is a strong correlation between the observed and predicted bedload transport rates but the observed rates were significantly lower. (B) Variation in excess stream power explains 90% of the variation in the "corrected" measured bedload transport rate.

are not accounted for in a general model. This makes the development of models that can predict sediment movement, even in relatively simple environments and situations such as the Miers Valley in Antarctica, difficult. However, as observed by others (Bagnold 1986; Martin and Church, 2000) excess stream power is able to explain a high percentage of the variation in bedload transport rates, once the observed transport rates are adjusted for depth and grain size, for a range of environments.

Conclusion

Even in this highly simplified environment considerable variability in the sediment transport rate was observed. While the observed bedload transport rate does relate to excess stream power (to the power of 1.5) as in the Bagnold equation, the Bagnold equation over-estimates the transport rate by a factor of five. An accurate predictive function was obtained only after making an empirical calibration using data specific to the current study and this limits its wider application. The relationship based on excess stream power was particularly useful at lower discharges and velocities. Other factors such as bedform migration, changes in bedform morphology, and sediment supply limit the predictive ability of transport formulae at higher discharges. The data from this study in Antarctica conforms, very well, to the observations made in quite different environments.

Acknowledgements

The University Grants Committee and the Internal Research Grants Committee of Victoria University of Wellington provided financial support for this research project. Logistic support was provided by the Antarctic Division of DSIR. The field assistance of Heather Campbell was greatly appreciated. The authors would also like to thank Malcolm Newson, Jonathon Laronne, and other referees for their useful comments that helped improve the manuscript.

References

Bagnold, R. 1980: "An empirical correlation of bed load transport rates in flumes and natural rivers." *Proceedings of the Royal Society, London Series A,* 372: 543-473.

Bagnold, R. 1986: "Transport of solids by natural water flow: evidence for a worldwide correlation." *Proceedings of the Royal Society, London Series A,* 405: 369-374.

Blank, H.R.; Cooper, R.A.; Wheeler, R.H.; Willis, I.A.G. 1963: "Geology of the Koettlitz-Blue Glacier region, Southern Victoria Land, Antarctica." *Transactions of the Royal Society of New Zealand – Geology,* 2(5): 79-100.

Campbell, H. 1990: Patterned ground, Miers Valley, Antarctica. Unpublished BSc (Hons) research project, Research School of Earth Sciences, Victoria University of Wellington, 76 p.

Garcia, C.; Laronne, J.; Sala, M. 2000: Continuous monitoring of bedload flux in a mountain gravel-bed river. *Geomorphology*, 34: 23-31.

Gomez, B.; Naff, R.; Hubbell, D. 1989: Temporal variations in bedload transport rates associated with the migration of bedforms. *Earth Surface Processes and Landforms*, 14: 135-156.

Gomez, B.; Church, M. 1989: An assessment of bed load sediment transport formulae for gravel bed rivers. *Water Resources Research*, 25: 1161-1186.

Hawke, R.M. 1990: Fluvial sediment transport in the Miers Valley, Antarctica. Unpublished BA (Hons) research project, Research School of Earth Sciences, Victoria University of Wellington, 101 p.

Helley, E.; Smith, W. 1971: *Development and calibration of a pressure-difference bedload sampler.* United States Geological Survey Open-file Report, 18 p.

Knighton, D. 1998: *Fluvial forms and processes: a new perspective.* Edward Arnold, London, 383 p.

Leopold, L.; Emmett, W. 1997: Bedload and river hydraulics inferences from the East Fork River, Wyoming. *US Geological Survey Professional Paper*, 1583, 52 p.

Martin, Y.; Church, M. 2000: Re-examination of Bagnold's empirical bedload formulae. *Earth Surface Processes and Landforms*, 25: 1011-1024.

McConchie, J.A.; Winchester, D.R.; Campbell, H.J.; Hawke, R.M. 1990: The hydrology, glaciology, and sediment transport processes of the Miers Valley (K046). *New Zealand Antarctic Record* 10(2): 23-25.

Mosley, P. 1988: Bedload transport and sediment yield in the Onyx River, Antarctica. *Earth Surface Processes and Landforms*, 13: 51-67.

Reid, I., Layman, J.; Frostick, L. 1980: The continuous measurement of bedload discharge. *Journal of Hydraulic Research*, 18: 243-249.

Reid, I.; Bathurst, J.; Carling, P.; Walling, D.; Webb, B. 1997: Sediment erosion, transport and deposition. In, Thorne, C., Hey, R.; Newson, M. (eds) *Applied fluvial geomorphology for river engineering and management*: 95-135.

Ryan, S.; Porth, L. 1999: A field comparison of three pressure-difference bedload samplers. *Geomorphology*, 30: 307-322.

Tunnicliffe, J.; Gottesfeld, A.; Mohamed, M. 2000: High resolution measurement of bedload transport. *Hydrological Processes*, 14: 2631-2643.

Thorne, C.; Hey, R.; Newson, M. 1997: *Applied fluvial geomorphology for river engineering and management.* John Wiley & Sons, Chichester, 376 p.

Manuscript received: 22 January 2001; accepted for publication: 30 March 2001.